Journal of Sound and Vibration (2001) **245**(5), 960–967
doi:10.1006/jsvi.2001.3578, available online at http://www.idealibrary.com on IDEAL®

DAMPING RATIO AND NATURAL FREQUENCY BIFURCATIONS IN ROTATING SYSTEMS

M. I. Friswell

Department of Mechanical Engineering, University of Wales Swansea, Swansea SA2 8PP, Wales.
E-mail: m.i.friswell@swansea.ac.uk

J. E. T. Penny

School of Engineering and Applied Science, Aston University, Birmingham B4 7ET, England

S. D. Garvey

School of Mechanical, Materials, Manufacturing Engineering and Management, Nottingham University, University Park, Nottingham NG7 2RD, England

AND

A. W. Lees

Department of Mechanical Engineering, University of Wales Swansea, Swansea SA2 8PP, Wales

(*Received* 20 *July* 2000, *and in final form* 14 *December* 2000)

1. INTRODUCTION

Campbell diagrams are very common in the analysis of rotating machines [1–4]. They show the variation of natural frequencies as a function of rotational speed. Typically, the natural frequencies change with speed because of gyroscopic effects and bearing characteristics. Usually, the topology of the Campbell diagram is very simple, particularly if the supports are isotropic and the rotor symmetric. The main purpose of this paper is to show that viscous damping in the bearings can produce bifurcations in both the Campbell diagram and the plot of damping ratio against shaft speed.

2. THE RIGID ROTOR

Consider the rigid rotor on flexible supports shown in Figure 1, where the co-ordinate origin is placed at the rotor centre of gravity. The Ox and Oy directions are orthogonal to the rotor axis and to each other. The stiffness at bearing 1 in the Ox direction is given by k_{x1}. The stiffness in the Oy direction and those at bearing 2 are defined in a similar, consistent way, as are the damping coefficients. The use of discrete springs and dashpots has implicitly assumed that the principal axes for both stiffness and damping are in the Ox and Oy directions. The equations of motion for this rotor, are [1–4]

$$\begin{aligned} m\ddot{u} + c_{xT}\dot{u} + c_{xC}\dot{\psi} + k_{xT}u + k_{xC}\psi &= 0,\\ m\ddot{v} + c_{yT}\dot{v} - c_{yC}\dot{\theta} + k_{yT}v - k_{yC}\theta &= 0,\\ I_d\ddot{\theta} + I_p\Omega\dot{\psi} - c_{yC}\dot{v} + c_{yR}\dot{\theta} - k_{yC}v + k_{yR}\theta &= 0,\\ I_d\ddot{\psi} - I_p\Omega\dot{\theta} + c_{xC}\dot{u} + c_{xR}\dot{\psi} + k_{xC}u + k_{xR}\psi &= 0, \end{aligned} \tag{1}$$

0022-460X/01/350960 + 08 $35.00/0

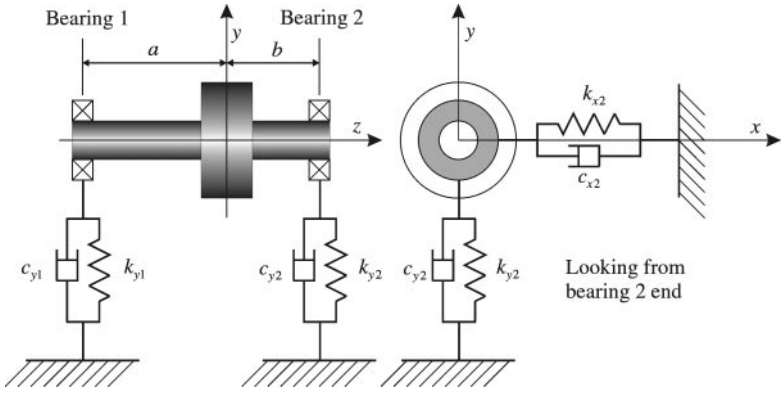

Figure 1. The rigid rotor on flexible supports.

where

$$\begin{aligned} c_{xT} &= c_{x1} + c_{x2}, & c_{yT} &= c_{y1} + c_{y2}, \\ c_{xC} &= -ac_{x1} + bc_{x2}, & c_{yC} &= -ac_{y1} + bc_{y2}, \\ c_{xR} &= a^2 c_{x1} + b^2 c_{x2}, & c_{yR} &= a^2 c_{y1} + b^2 c_{y2} \end{aligned} \tag{2}$$

and the stiffness coefficients are defined in a similar way. u and v are the displacements in the Ox and Oy directions, and θ and ψ are the rotations about the Ox and Oy axes. a and b are the distances between the rotor centre of gravity and the bearings, as shown in Figure 1. The subscripts T and R represent the combined translational and rotational stiffnesses of the bearings referred to the co-ordinate origin. The subscript C represents the coupling between the translational and rotational degrees of freedom.

For simplicity we will only analyze the case when the translational and rotational degrees of freedom decouple, so that $k_{xC} = k_{yC} = 0$ and $c_{xC} = c_{yC} = 0$. Thus equation (1) becomes

$$\begin{gathered} m\ddot{u} + c_{xT}\dot{u} + k_{xT}u = 0, \qquad m\ddot{v} + c_{yT}\dot{v} + k_{yT}v = 0, \\ I_d\ddot{\theta} + I_p\Omega\dot{\psi} + c_{yR}\dot{\theta} + k_{yR}\theta = 0, \\ I_d\ddot{\psi} - I_p\Omega\dot{\theta} + c_{xR}\dot{\psi} + k_{xR}\psi = 0. \end{gathered} \tag{3}$$

We now consider two particular cases of damping.

3. RIGID ROTOR ON ISOTROPIC SUPPORTS WITH DAMPING

We consider the case of a rigid rotor on isotropic supports, that is where the support stiffness and damping are the same in both the x and y directions. Thus, we can let $k_{xT} = k_{yT} = k_T$, $c_{xT} = c_{yT} = c_T$, and similarly for the angular quantities. Equation (3) becomes

$$\begin{gathered} m\ddot{u} + c_T\dot{u} + k_T u = 0, \qquad m\ddot{v} + c_T\dot{v} + k_T v = 0, \\ I_d\ddot{\theta} + I_p\Omega\dot{\psi} + c_{yR}\dot{\theta} + k_R\theta = 0, \\ I_d\ddot{\psi} - I_p\Omega\dot{\theta} + c_R\dot{\psi} + k_R\psi = 0. \end{gathered} \tag{4}$$

Combining the first and second, and third and fourth equations by letting $r = u + jv$ and $\phi = \psi - j\theta$, we have

$$m\ddot{r} + c_T\dot{r} + k_T r = 0, \qquad I_d\ddot{\phi} - jI_p\Omega\dot{\phi} + c_R\dot{\phi} + k_R\phi = 0. \tag{5}$$

This double use of the imaginary unit for both temporal and spatial phases is consistent in this case because we are only considering the synchronous response. Looking for eigenvalues by setting $r(t) = r_0 e^{st}$ and $\phi(t) = \phi_0 e^{st}$ in equation (5) gives

$$[ms^2 + c_T s + k_T]r_0 = 0, \qquad [I_d s^2 + (c_R - jI_p\Omega)s + k_R]\phi_0 = 0. \tag{6}$$

The first of equation (6) has, if $2k_T > c_T^2$, the complex conjugate pair of roots,

$$s_{1,2} = -\frac{c_T}{2m} \pm j\sqrt{\frac{k_T}{m} - \frac{c_T^2}{2m}}. \tag{7}$$

The roots of the second of equation (6) cannot be expressed as a simple algebraic equation with a real and an imaginary part. However, the two roots will be of the form

$$s_3 = -\zeta_3\omega_3 - j\omega_{d3} \quad \text{and} \quad s_4 = -\zeta_4\omega_4 + j\omega_{d4}, \tag{8}$$

where $\omega_{d3} = \omega_3\sqrt{1-\zeta_3^2}$ and $\omega_{d4} = \omega_4\sqrt{1-\zeta_4^2}$, and ζ_3, ζ_4, ω_3 and ω_4 are all positive. Thus we have

$$[s - (-\zeta_3\omega_3 - j\omega_{d3})][s - (-\zeta_4\omega_4 + j\omega_{d4})] = 0 \tag{9}$$

or expanding,

$$s^2 + [(\zeta_3\omega_3 + \zeta_4\omega_4) - j(\omega_{d4} - \omega_{d3})]s + [(\zeta_3\zeta_4\omega_3\omega_4 + \omega_{d3}\omega_{d4}) + j(\omega_{d3}\zeta_4\omega_4 - \omega_{d4}\zeta_3\omega_3)] = 0. \tag{10}$$

Examining equation (6) we see that the constant term in the second of equation (6) is real. Thus in equation (10) the imaginary part of the constant term must be zero. Hence

$$\omega_{d3}\zeta_4\omega_4 - \omega_{d4}\zeta_3\omega_3 = 0. \tag{11}$$

Thus, it follows that

$$\omega_3\omega_4\zeta_4\sqrt{1-\zeta_3^2} = \omega_3\omega_4\zeta_3\sqrt{1-\zeta_4^2} \tag{12}$$

and hence $\zeta_3 = \zeta_4$.

This tells us that even when a pair of natural frequencies separate due to gyroscopic effects, the damping factor for the two modes will be identical if the bearings are isotropic.

4. RIGID ROTOR WITH ANISOTROPIC DAMPING IN SUPPORTS

We now consider the situation that arises when the support stiffnesses are identical in the Ox and Oy directions but the damping is not. Thus in equations (3) we set $k_{xT} = k_{yT} = k_T$

and $k_{xR} = k_{yR} = k_R$. Thus equations (3) become

$$m\ddot{u} + c_{xT}\dot{u} + k_T u = 0, \qquad m\ddot{v} + c_{yT}\dot{v} + k_T v = 0,$$

$$I_d\ddot{\theta} + I_p\Omega\dot{\psi} + c_{yR}\dot{\theta} + k_R\theta = 0,$$

$$I_d\ddot{\psi} - I_p\Omega\dot{\theta} + c_{xR}\dot{\psi} + k_R\psi = 0. \tag{13}$$

The first and second equations of (13) are uncoupled and can readily be solved independently. Focusing our attention of the second pair of coupled equations, we will look for eigenvalues by setting $\theta = \theta_0 e^{st}$ and $\psi = \psi_0 e^{st}$. Thus, the second pair of equations of (13) becomes

$$(I_d s^2 + c_{yR}s + k_R)\theta_0 + I_p\Omega s\psi_0 = 0,$$

$$(I_d s^2 + c_{xR}s + k_R)\psi_0 - I_p\Omega s\theta_0 = 0. \tag{14}$$

The characteristic equation corresponding to equation (14) is

$$(I_d s^2 + c_{yR}s + k_R)(I_d s^2 + c_{xR}s + k_R) + I_p^2\Omega^2 s^2 = 0. \tag{15}$$

This can be rearranged to give

$$(I_d s^2 + c_{mR}s + k_R)^2 = (c_{dR}^2 - I_p^2\Omega^2)s^2, \tag{16}$$

where $c_{mR} = (c_{xR} + c_{yR})/2$ and $c_{dR} = (c_{xR} - c_{yR})/2$. Now if $\Omega^2 < c_{dR}^2/I_p^2$ the right-hand term is positive. Letting $\alpha^2 = c_{dR}^2 - I_p^2\Omega^2$, and taking the square root of equation (16) gives

$$I_d s^2 + (c_{mR} \pm \alpha)s + k_R = 0. \tag{17}$$

Clearly if $\Omega^2 < c_{dR}^2/I_p^2$ then the natural frequencies of the two forms of equation (17) are equal but the damping coefficients, and hence the damping ratios, are different depending on whether we take $(c_{mR} + \alpha)$ or $(c_{mR} - \alpha)$. When $\Omega = 0$, $(c_{mR} \mp \alpha)$ simplifies to c_{xR} and c_{yR}. As Ω increases, α tends to zero, and both damping coefficients tend towards c_{mR}.

If $\Omega^2 > c_{dR}^2/I_p^2$ the right-hand side of equation (16) is negative and we can define a transformed speed, $\hat{\Omega}$, by

$$I_p^2\hat{\Omega}^2 = I_p^2(\Omega^2 - (c_{dR}/I_p)^2). \tag{18}$$

The characteristic equation (16) may be written as

$$(I_d s^2 + c_{mR}s + k_R)^2 + I_p^2\hat{\Omega}^2 s^2 = 0. \tag{19}$$

Consider now the third and fourth equations of (4). These equations describe the case when both the support stiffness and the damping are isotropic. Letting $\psi(t) = \psi_0 e^{st}$ and $\theta(t) = \theta_0 e^{st}$ in these equations produces

$$(I_d s^2 + c_R s + k_R)\theta_0 + I_p\Omega s\psi_0 = 0,$$

$$-I_p\Omega s\theta_0 + (I_d s^2 + c_R s + k_R)\psi_0 = 0, \tag{20}$$

which gives the characteristic equation

$$(I_d s^2 + c_R s + k_R)^2 + I_p^2 \Omega^2 s^2 = 0 \tag{21}$$

Comparing equations (19) and (21) we see that when $\Omega^2 > c_{dR}^2/I_p^2$, the anisotropic damping case will give same pattern of behaviour as isotropic case, except that the behaviour is dependant on the mean, rather than the actual damping coefficients and the frequency is shifted from Ω to $\hat{\Omega}$.

Thus, for rotor speeds less than c_{dR}/I_p the natural frequencies corresponding to the rotational degrees of freedom are equal, and the damping ratios are different. For rotor speeds greater than c_{dR}/I_p these natural frequencies separate but the damping ratios are equal.

5. A SIMPLE EXAMPLE

A uniform rigid rotor has a length of 0·5 m and a diameter of 0·2 m and is made from steel having a density of 7810 kg/m^3. It is supported at its ends by bearings. Both bearings supports have horizontal and vertical stiffnesses of 1 MN/m. The damping coefficient in the Ox direction is 1 kN s/m and in the Oy direction, 1·2 kN s/m. The eigenvalue problem is solved from rest to a maximum rotor speed of 500 r.p.m. Figure 2 shows the variation of natural frequency with rotor speed, and Figure 3 shows the variation of the damping ratio. Note that the damping ratios of the two rotational modes become identical at 194·60 r.p.m. Also, at this speed the natural frequencies separate.

6. A COMPLEX EXAMPLE

The above analysis was performed for a simple rotor system. Similar effects can occur with more complex rotor systems. Figure 4 shows a schematic of a flexible rotor supported on two fluid bearings located at the ends of the shaft. The shaft is 1·5 m long, 50 mm in diameter and is modelled using 6 Timosenko beam elements. One disc of 70 mm thickness

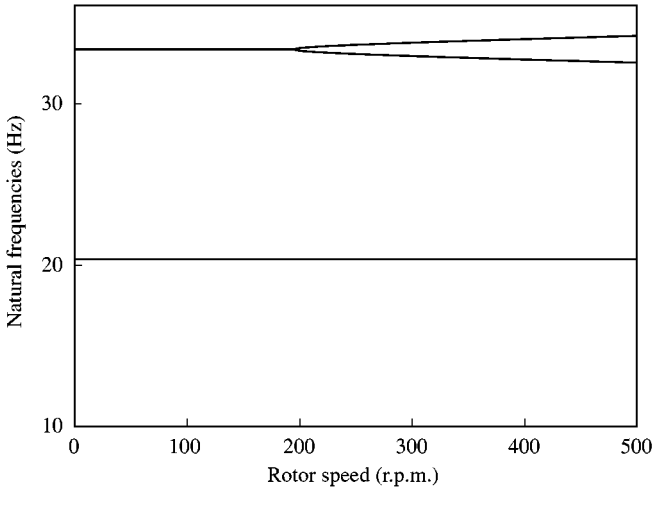

Figure 2. Plot of natural frequencies against rotor speed for each mode for the rigid rotor example.

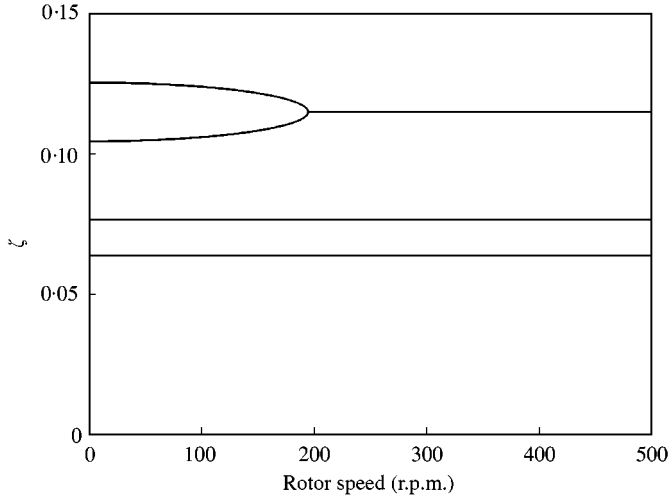

Figure 3. Plot of damping ratios against rotor speed for each mode for the rigid rotor example.

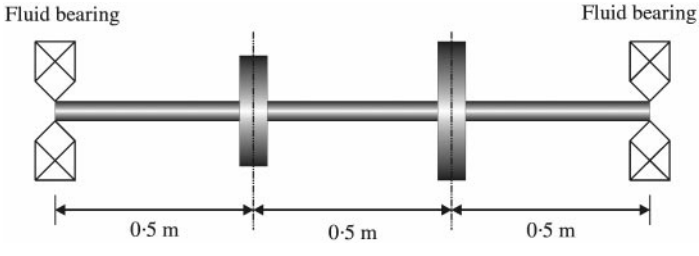

Figure 4. The flexible rotor on fluid bearings.

and 280 mm diameter is placed 0·5 m from the left bearing, and a second disc of 70 mm thickness and 350 mm diameter is placed 0·5 m from the right bearing. The fluid bearings have a diameter of 100 mm, a length of 55 mm, a clearance of 0·1 mm and are filled with oil of viscosity 0·015 N s/m^2. Short bearing theory [5] is used to compute the linearized stiffness and damping matrices for the bearings, and these are shown in Figures 5 and 6. The load on each bearing is taken as 450 N. Figures 7 and 8 show the variation of natural frequency and damping ratio of modes 5 and 6 of the rotor. The bifurcations at 408 r.p.m. are quite clear, although the damping ratio does not remain equal when the natural frequencies separate because the bearing stiffness and mass matrices are asymmetric. Furthermore, for low rotor speeds the natural frequencies are close, but not equal, and the damping ratios do not quite become equal.

7. CONCLUSIONS

This paper has investigated how the variation of natural frequency and damping ratio change with rotational speed for rotating machines. Rigid rotors on anisotropic flexible supports are studied in detail for the case when there is no coupling between the translational and rotational degrees of freedom. At low speed the natural frequencies corresponding to the rotational degrees of freedom are equal, and the damping ratios are

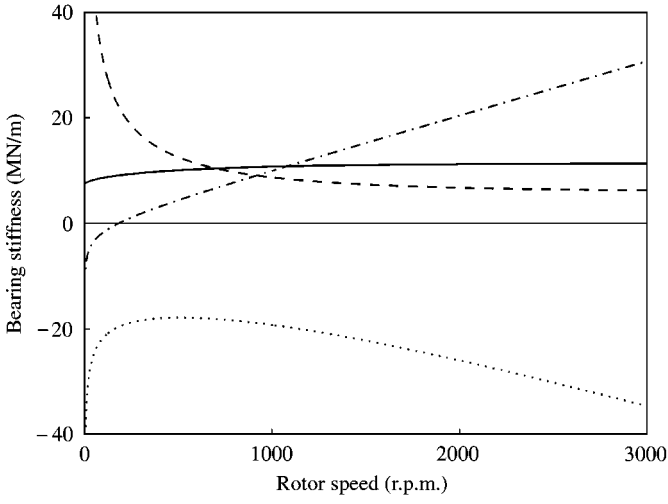

Figure 5. The speed-dependent stiffness parameters for the fluid bearings (y is vertical): ——, k_{xx}; - · - ·, k_{xy}; · · · ·, k_{yx}; - - -, k_{yy}.

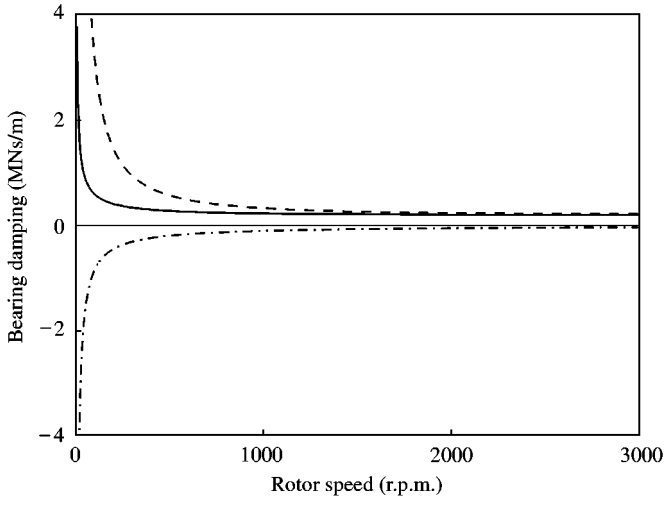

Figure 6. The speed-dependent damping parameters for the fluid bearings (y is vertical): ——, c_{xx}; - · - ·, $c_{xy} = c_{yx}$; - - -, c_{yy}.

different. For high rotor speeds these natural frequencies separate but the damping ratios are equal. These features are not so apparent for more complex systems; however, the knowledge that such features can exist should be reassuring when faced with unusual features in these plots of natural frequency and damping ratio.

ACKNOWLEDGMENTS

Professor Michael Friswell acknowledges the support of the EPSRC through the award of an Advanced Fellowship.

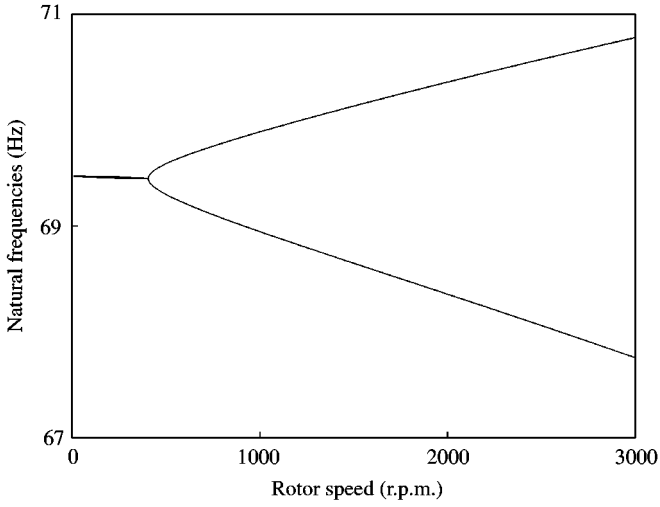

Figure 7. Plot of natural frequencies against rotor speed for modes 5 and 6 for the fluid bearing example.

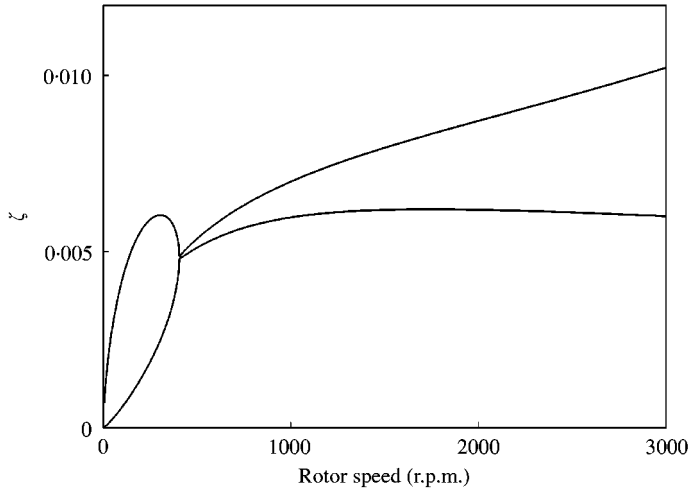

Figure 8. Plot of damping ratios against rotor speed for modes 5 and 6 for the fluid bearing example.

REFERENCES

1. A. D. DIMARAGONAS and S. A. PAIPETIS 1983 *Analytical Methods in Rotor Dynamics*. London: Elsevier-Applied Science.
2. E. KRÄMER 1993 *Dynamics of Rotors and Foundations*. Berlin: Springer-Verlag.
3. J. S. RAO 1983 *Rotor Dynamics*. New York: John Wiley and Sons.
4. M. LALANNE and G. FERRARIS 1998 *Rotordynamics Prediction in Engineering*. Chichester. John Wiley and Sons: second edition.
5. D. M. SMITH 1969 *Journal Bearings in Turbomachinery*. London: Chapman and Hall.